Research Article

Multi-attribute optimization of EDM process parameters for machining of SiC and B4C particle reinforced Al 6061 metal matrix composite adopting TOPSIS method

Anil Kumar Bodukuri[1*] and Eswaraiah Kesha[2]
Research scholar, Kakatiya University, Warangal, Telangana, India[1]
Professor, Kakatiya Institute of Technology and Science, Warangal, Telangana India[2]

Abstract
The tendencies of using composite materials are increasing rapidly in advanced engineering and technology applications. Ceramic reinforced aluminum composites are difficult to machine by conventional machining processes. In this work, ceramic reinforced aluminum composites are machined by Electric Discharge Machine (EDM). The goal of this study is to focus on the influence of EDM settings on Al6061 Metal Matrix Composite (MMC) reinforced with Silicon Carbide (SiC) and Boron Carbide (B4C) particles. The MMC is prepared by stirring casting route, then the workpiece is mounted on the electric discharge machine to perform the machining. Because MMC contains high abrasive ceramic (SiC and B4C) particles that are difficult to machine using traditional machining methods, an electrical discharge machine is used for machining. The experiments were conducted with four process parameters like Pulse current (I), Pulse off Time (P-Off), Pulse on Time (P-On), and Tool Lift (TL) with three levels in each parameter to examine the response measures such as Material Removal Rate (MRR), Surface Roughness (SR), Tool Wear Rate (TWR) and Surface Crack Density (SCD). The experimental results reveal that the surface crack density, MRR, SR, and TWR increases with an increase in current and pulse in time. The optimal combinations of process parameters were identified. Obtained optimal machining conditions are I input level at 9 Amps, P-On input level at 20 µs, P-Off input level at 50 µs, and Tool Lift input level at 4.5 µs with results of 0.103g/min MRR, 0.022 g/min TWR, 4.108µm SR and 0.0048 µm SCD.

Keywords
Composite material, MRR, SR, Optimization, TOPSIS, Unconventional machining, EDM.

1.Introduction
A composite material is defined as a material that is made up of at least two or more constituent materials. These constituent materials have remarkably different physical and chemical properties, and when combined, they form a material with characteristics not found in the individual constituents [1]. Composite materials are typically made up of two phases: matrix and reinforcement. If the matrix phase is considered with metal or alloy and in the reinforcement phase two or more materials are used, then it is known as Hybrid Metal Matrix Composite (HMMC). The tendencies of using HMMC materials are increasing rapidly in modern engineering applications such as space, aircraft, automotive industries, defense, and nuclear fields.

The addition of ceramic reinforcements in the metal matrix results in a composite material with high specific strength and hardness [2]. HMMC materials are challenging to machine using traditional methods due to their high reinforced strength, so the machining of these HMMC's is usually done by non-traditional machines. Electric Discharge Machine (EDM) is an unconventional machine used for machining materials possessing high hardness and specific strength like superalloys, Metal Matrix Composite (MMC) and HMMC [3]. The background of the EDM process began with Joseph Priestly's findings in 1770. In his investigations, it is observed that electrical discharges had eroded material from the electrodes. Lazarenko, the Soviet researcher, invented a machining technology that became the cornerstone for contemporary EDM in 1940. The basic principle of EDM is simple. A gap is maintained between an electrode and a workpiece, and an electrical spark is formed in this gap. The movement of electricity is

---

apparent in the form of a spark with temperatures ranging from 8000 to 12000 0C, this electric spark generates a lot of heat that causes, melting and even evaporation of material from the tool and workpiece. The spark is precisely regulated and focused so that it only touches the material's surface. The heat treatment underneath the surface is largely unaffected by the EDM procedure. When using EDM, the spark is always created in a dielectric medium. The dielectric fluid serves as a coolant and flushes away the eroded metal particles [4].

The main objectives of this article are as under:
1. Selection of work sample which has superior properties for modern engineering applications.
2. Selection of a non-conventional machine, EDM for machining components. Selection of machining parameters of the EDM through Design of Experiments (DOE).
3. Performing experiments and analyzing the data
4. Finding the optimal machining conditions by a proper optimization technique.
5. Prediction and validation of data.

2.Literature review

In a hybrid metal matrix composite, Al 6061 was used as the matrix material, and two ceramic reinforcements, Silicon Carbide (SiC) and Boron Carbide (B4C), were used in appropriate proportions. Based on mechanical properties, an appropriate composition (90 weight percent of Al-6061, 7 weight % of B4C, and 3 weight % of SiC) was recommended after examining various combinations of B4C, SiC, and Al6061. Because of the presence of B4C (the third hardest material) and SiC ceramic reinforcements, MMC materials are hard [5].

Aluminum alloys reinforced with nano B4C have a higher dislocation density than monolithic alloys, as seen in TEM images. The addition of nano B4C to an aluminum alloy matrix increased its tensile strength and hardness while maintaining its impact resistance and ductility [6].

A stir casting course was chosen for the preparation of ZrO_2- Al MMCs. They included distinct weight rates of ZrO_2 in the range of 0 to 10 wt. percent in the Al6061 matrix. They discovered that as weight levels increased, mechanical property estimations improved while elongation decreased [7].

A Non-Conventional EDM was considered for machining the prepared MMC. The EDM process is a novel machining technique in which the material is

eroded as a result of the Transformation of electrical to thermal energy by a series of several electrical discharges that occur between the work sample and tool electrode, both of which are immersed in a dielectric medium and separated by a small gap [8].

The mechanical properties of Al-MMC is influenced by the weight percent of adding reinforcements, followed by stirrer speed, time, and temperature of the stir casting process [9].

In performance measures such as Material Removal Rate (MRR), Surface Roughness (SR), Tool Wear Rate (TWR) and Surface Crack Density (SCD), EDM machining of tungsten carbide with a cooper tool result in less surface cracks and TWR [10].

In the EDM process, a servo system maintains a small gap between the workpiece and the tool, ranging from 0.025 to 0.03 mm. TWR and MRR were improved by increasing the pulse on time and pulse current during EDM machining of Al-SiC composite [11].

In ceramic reinforced composites, SiC particles protect and conceal the MMC workpiece from electric discharges in EDM and reduce MRR, SR, and TWR [12].

Taguchi DOE and analysis exhibits optimum combination parameters for a single response in a set of input independent machining parameters [13].

The Data Envelopment Analysis Ranking (DEAR) approach was found to be an effective method of multi-objective optimization in two case study problems [14].

When using Technique of Order Preference Similarity to the Ideal Solution (TOPSIS) to perform multi-objective optimization of Ti alloy, the Taguchi method was used, and it was discovered that increasing process parameters like pulse on time and pulse current improved performance measures [15].

MMC materials are challenging to machine using traditional methods due to their high reinforced strength, so the machining of these MMC's is usually done by non-traditional machines [16].

Liquid and solid phase techniques can be used to create composite materials. In HMMC, Al 6061 was used as the matrix material and two ceramic reinforcements, SiC and B4C, were used in

appropriate proportions to obtain superior properties to monolithic Al alloy [17, 18].

A typical stir casting procedure was used to create an aluminum-based MMC with an AA6061 alloy configuration and reinforcement of 1.5 wt percent SiC and B4C [19].

The Al reinforced with SiC and B4C particle reinforced exhibited improved mechanical properties such as impact, tensile strength, hardness, and flexural strength when compared to monolithic Al alloy. [20, 21].

Al-SiC MMC is commonly used in dies, parts, and products in the aerospace, electronics, military, automotive, and medical industries. V, IP, Duty Factor, and Ton were the control parameters used during the machining MMC on EDM. The material removal rate is optimal and the surface roughness is excellent when the current is high and the voltage is low [22].

The Taguchi method and DEAR were used to optimize the process input parameters on TiB2 reinforced Al7075 MMC in the AWJM process [23].

TOPSIS and Grey Relational Analysis (GRA) with Taguchi were investigated for ED machining of H-11 Die steel with electrolytic copper and the effectiveness of multi-attribute optimization was evaluated [24].

DEAR with the Taguchi method was revealed that the optimal set of input parameters in an efficient way [25].

To improve performance measures like MRR, SR, TWR, surface integrity factors, and Kerfs width, machining parameters such as pulse off time, servo voltage, wire tension, pulse current, wire-speed, and pulse on time can be used. The Taguchi, GRA Response Surface Methodology (RSM), and Analysis of Variance (ANOVA) are used for analysis of various materials such as steel alloys, nickel superalloys, and MMCs [26].

Scientists and practitioners have given Multi-objective Decision-Making techniques a lot of thought in terms of identifying, analyzing, and placing options via various technologies. TOPSIS continues to perform admirably in a variety of application areas [27].

Tribological properties were vital for Al 6061-based HMMCs reinforced with B4C and SiC ceramics. The presence of ceramic Reinforcements increased the coefficient of friction at higher sliding speeds. Oxidation, adhesion, and abrasion were identified as the main wear mechanisms, and these were confirmed using Field Emission Scanning Electron Nicroscope (FESEN) and Energy-dispersive Spectroscopy (EDS) on worn-out specimens [28].

The morphology of the surface layer was examined using Scanning Electron Microscope (SEM), and the chemical composition was investigated using Energy-Dispersive X-ray Spectroscopy (EDX). The ideal machining settings for the best-machined surface quality and the narrowest kerf width were determined for precision machining [29].

The machining parameters for surface roughness optimization have been attempted. Confirmation tests were conducted to test the model, and the predicted results were found to be very close to the experimental data. The surface morphology of machined surfaces has also been studied using SEM. Several surface flaws and their causes have been discovered [30].

For LM6-Alumina stir casted MMC, the EDM Machining parameters are optimised to achieve the best MRR, reduced SR, and TWR. Multiple performance characteristics are designed and optimised using grey relation analysis. The discharged current, according to the findings, is the most important factor influencing surface finish and material removal rate [31].

Al MMC is made using a stir casting method with three different weight percentages of B4C and Gr reinforcements. The prepared sample is then machined on an EDM for optimal response optimization of EDM process parameters. The Wear Ratio (WR) decreases initially with Ton and increases with an increase in reinforcement percentages. The formation of a ceramic layer between the tool and the workpiece causes a decrease in WR in a nonlinear style [32].

EDM is used to machine MMCs to find the best process parameters. The most influencing parameter for MMC machining is current, polarity, and followed by T-on and gap voltage due to the availability of high temperature generated by series of sparks by EDM [33].

An in-depth examination was conducted to determine the impact of process parameters on response parameters. It has been reported that MRR and TWR

are mostly influenced by current, polarity and followed by T-on due to high temperature [34].

The machining of Al-B4C MMC was performed on vibration-assisted EDM to increase the performance of process parameters on responses. Current and tool vibration was the most influential parameter for MRR, SR, and flushing pressure for TWR [35].

The machining of Al/Cu/Ni on EDM was employed and it is analyzed that the current is the most significant parameter followed by T On, Toff, and Current Peak (CP) on the surface quality of the machined sample [36].

The effectiveness of optimum input parameters of EDM on die steel was evaluated. The TOPSIS multi-objective optimization was employed to recognize the optimum process parameters to achieve excellent surface quality and MRR with a low-frequency vibration tool [37].

ECDM was used to machine the Al6063-SiC MMC. The results show that when high Ton is used for longer than 3 ms, the generation of heat decreases and the MRR decreases. The intermittent gas film collapses, causing electrical discharges to be hampered [38].

Al-SiC-Gr MMC was prepared by stir casting method and machining was performed on MMC by EDM. The most impacting parameter on MRR responses of Al-SiC- Gr workpiece on EDM has been reported as current and T On. T Off has less significance on MRR [39].

The machining of high hardened materials, including MMC by EDM is easy and efficient. The attempt was made to machine SiC-Al MMC in which more than 50% of SiC was reinforced. Due to the high ceramic quantity in MMC while machining it forms a shielding layer in the spark gap. Particle Swarm Optimization (PSO) and Support Vector Regression (SVR) hybrid optimization was employed to find the optimal process parameters of EDM. It has been recorded that as current and T On increases MRR and surface roughness increases due to the availability of high thermal energy [40].

Based on a literature review, the background and motivation for this work are to prepare and machine a novel HMMC with superior properties that can serve modern engineering applications. This article focuses on finding the optimum machining parameters to develop the quality and lifetime of the component

made by HMMC. This novel HMMC was made with Al 6061 as matrix material and reinforcement materials 3% SiC and 7 % B4C was considered for fabrication of workpiece. This novel HMMC is difficult to machine by convention methods as they possess high hard and abrasive ceramic particles like SiC and B4C. Hence a non-convention machine, EDM was considered for machining of this HMMC. According to the literature review, the majority of the work is done on MMC using wire EDM; however, it is understood that few researchers attempted machining of Hybrid MMC using Die-Sink EDM, and no work has been reported on multi-attribute optimization with TOPSIS method for machining of a novel based Al6061 reinforced SiC and B4C Hybrid MMC on EDM. Here TOPSIS aided with the Taguchi method has been used to find the optimal input machining parameters for better process parameters.

3.Methods and materials

The purpose of this paper is to discuss the preparation and machining of novel HMMC. EDM machining of HMMC to reduce manufacturing time, SR roughness, and SCD level, thereby increasing component service life in key applications. To prepare the HMMC Work sample, the stir casting method is used. The experimental run and test flowchart are depicted in *Figure 1*.
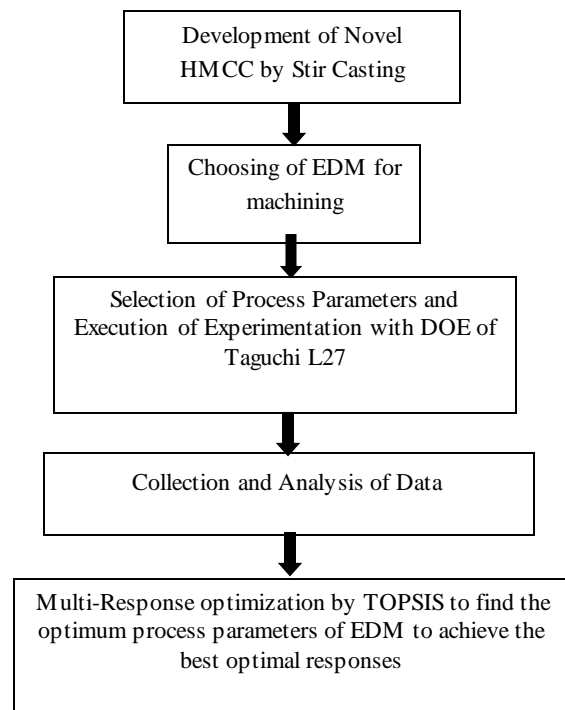
Figure 1 Flow chart

3.1 Development of work sample

The stir casting method was used to prepare the Hybrid MMC. Based on mechanical and physical properties, a pilot experiment was conducted to determine the appropriate reinforcement percentage. *Table 1* shows the Al-6061 Chemical composition. The matrix phase was chosen to be Al 6061 alloy, with particulate phase reinforcement consisting of 7% B4C and 3% SiC by weight. *Table 2* lists the mechanical and thermal properties of SiC and B4C. Initially, the chemical composition of Al 6061 billet was confirmed by spectroscopic examination, and the results were tabulated.

Table 1 Al-6061 Chemical composition

Elements	Composition (wt. %)
Magnesium	0.8-1.2
Iron	Max. 0.7
Silicon	0.4 – 0.8
Zinc	Max. 0.25
Copper	0.15-0.40
Manganese	Max. 0.15
Titanium	Max. 0.15
Chromium	0.04-0.35
Others	0.05
Aluminum	Balance

Table 2 Properties of SiC and B4C

Mechanical & Thermal Properties	SiC	B4C
Density	3.21 gm/cc	2.51 gm/cc
Melting Point Temperature	2760 °C	2450 °C
Elastic Modulus	410 GPa	362 GPa
Hardness (Vickers)	2800 Kg/mm2	3810 Kg/mm2
Tensile strength	210-370 MPa	261 MPa
Fracture Toughness KIC	3.2 MPa•m1/2	3 MPa•m1/2
Thermal Conductivity	115 W/m•°K	17 W/m•°K
Coefficient of Thermal Expansion	4.0×10^{-6} /°C	4.6×10^{-6} /°C

Al6061 alloy billet is made into small rectangular shaped parts to achieve a larger surface area for absorbing the heat and thus melts quickly. Then after it is inserted in a crucible and heated to melt in a stir casting furnace. To achieve proper melting the billet is heated up to 800oC and maintained for 30 minutes. Dry argon gas is passed into the furnace for the degasification of molten metal. Now the preheated ceramics 3 wt % of SiC particles of size 45 microns and 7 wt % of B4C particles of size 63 microns at 400 ºC were inserted through the provision of a stir casting furnace. The stirring action was done for 25 minutes for achieving uniform distribution of reinforcements in the matrix phase. The molten material is now poured into cylindrical molds. Molds were allowed to solidify at room temperature for 5 hours. The uniform distribution of reinforcements in the matrix phase is identified by SEM analysis and the SEM image is shown in *Figure 2*.
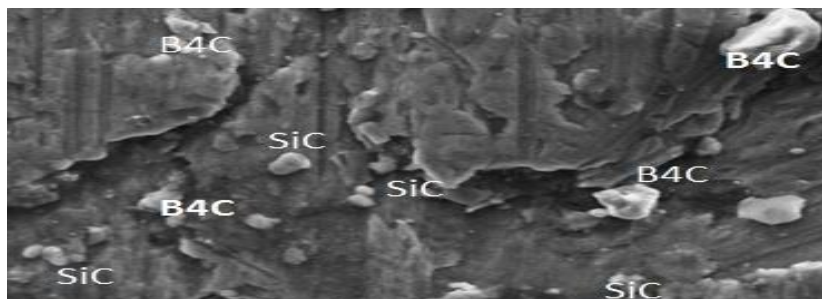

Figure 2 SEM image showing Uniform distribution of reinforcements in Al matrix

3.2 EDM and its mechanism

EDM consists of two electrodes, one electrode is connected to the tool and the other electrode is connected to the work sample. These two electrodes are separated with a small gap and always this gap is kept constant by the servo controller with the help of a feedback mechanism. The two electrodes are submerged in a dielectric fluid and they are connected to a programmable circuit power supply, this is known as the ignition phase which is shown in *Figure 3*. A closed circuit is formed when the voltage exceeds the breakdown voltage and sparks are produced in the dielectric fluid. This is known as the generation of plasma phase, which is shown in *Figure 3*. In this phase, high pressure and temperature are generated and this plasma is maintained for some time known as a pulse on time. After this phase suddenly plasma breaks down, which makes the molten materials at both tool and work surface boil violently and small droplets of liquid metal are ejected from the molten metal pool. This phase is known as melting and evaporation and is shown in *Figure 3*. The material eroded (debris) from two electrodes tool and work surface are flushed away by the dielectric fluid. The mechanism of the EDM process is shown in *Figure 3*.

A Nonconventional V3525 Askar Microns Die-Sink EDM was considering for machining of Al- Hybrid MMC. The selected die sink EDM is shown in *Figure 4*. The specification of EDM is shown in *Table 3*. Electrolytic copper was considered a tool with a 10 mm diameter. The EDM 30 oil was used as a dielectric medium during machining. It is also used for flushing debris or eroded material from tool and work surfaces.
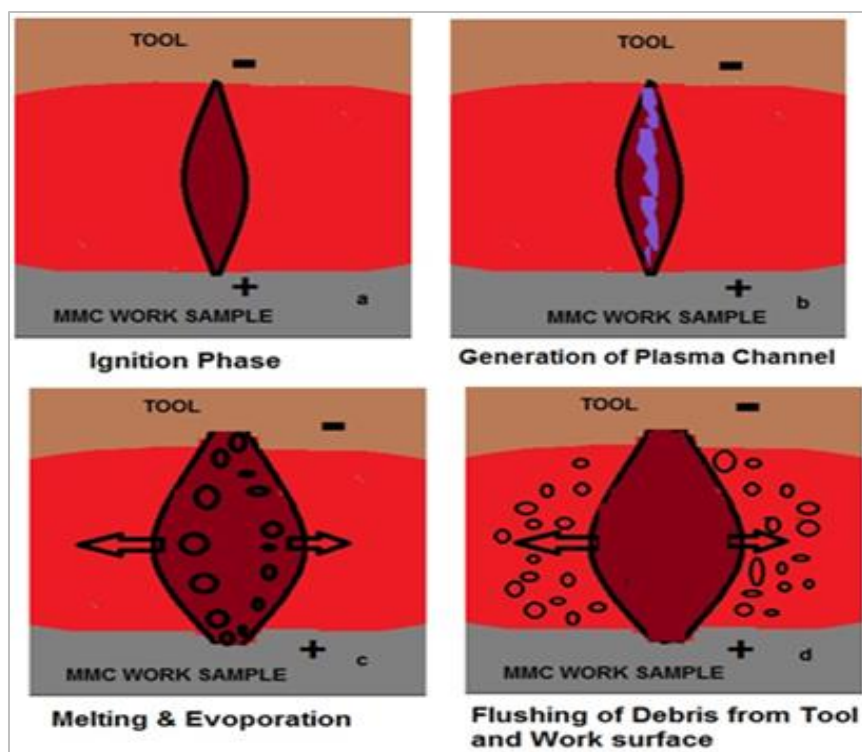
Figure 3 Mechanism of EDM process

Table 3 Specifications of EDM

EDM Mechanism	Melting & evaporation
Spark gap	0.010-0.500 mm
Peak voltage	30-250 V
Spark frequency	200-500 kHz
Workspace Dimensions	$600 \times 390 \times 275$ mm^3
Table Dimension	350×250 mm^2
Table loading	200 Kg
Dielectric medium	EDM 30-grade oil

3.3Selection of process parameters

Initially, a series of experiments were done on a work sample on EDM with copper toll to recognize the influence of input factors and their levels. The parameters and their levels are tabulated in *Table 4*.

Table 4 Parameter settings and their Levels

Input Parameters (Units)	Levels		
	1	2	3
I (Pulse Current) (A)	9	12	15
P-On (Pulse on time) (µs)	20	50	100
P-Off (Pulse off time) (µs)	50	100	200
TL (Tool Lift) (µs)	1.5	3	4.5

Figure 4 Electric discharge machine

3.4Experimentation and data collection

The hybrid MMC samples were mounted on EDM for machining with various input parameters and levels. Before machining the surfaces of the work sample and the tool were grounded by emery papers to obtain a good surface finish of 1 µm. Experiments were executed based on Taguchi DOE L29 orthogonal array. TWR, SR, MRR and SCD were treated as response characteristics and input machining parameters as I, P-On, P-Off, and TL and all the parametric values are presented in *Table 5*. MRR and TWR are evaluated by *Equations 1 and 2* respectively. SR values are obtained by The Mitutoyo SJ-210-

Series Portable Surface Roughness Tester shown in *Figure 5*. SCD was calculated by ZESIS SEM image analyzer software, *Figure 6* and *Figure 7* shows the SCD for experimental run 3 and 14.

$$MRR = \frac{(W1 - W2)mg}{T \min} \tag{1}$$

$$TWR = \frac{(T1 - T2)mg}{T \min} \tag{2}$$

W1, W2, T1, and T2 are the weights of the work sample and tool former and later machining with a digital balance in milligrams respectively and T is the time taken for machining in minutes.

Anil Kumar Bodukuri and Eswaraiah Kesha
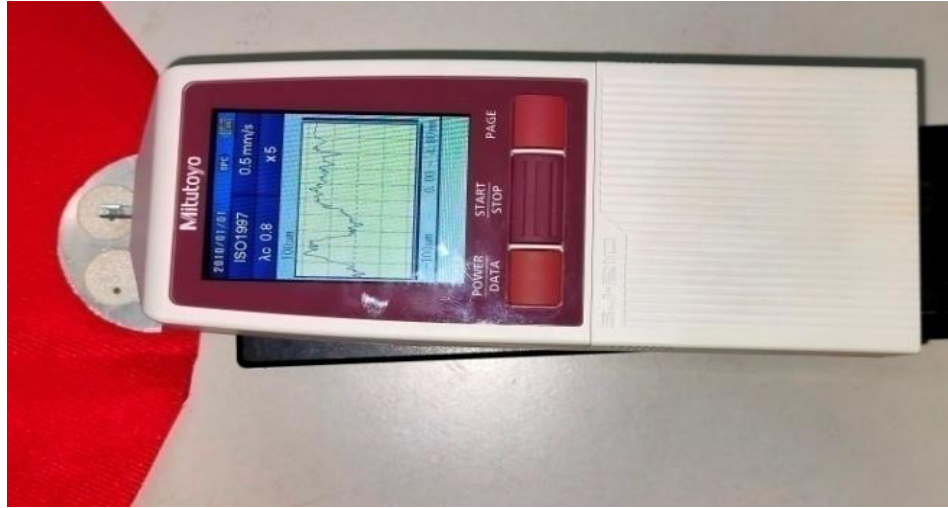
Figure 5 Mitutoyo SJ-210 series surface roughness tester

Table 5 Taguchi orthogonal array L27

EXP No	I (A)	P-On (µs)	P-Off (µs)	T L (µs)	MRR	TWR	SR	SCD
1	1	1	1	1	0.106	0.023	4.25009	0.006042
2	1	1	2	2	0.103	0.030	4.28688	0.005677
3	1	1	3	3	0.092	0.023	4.09385	0.004245
4	1	2	1	2	0.108	0.034	4.44577	0.006331
5	1	2	2	3	0.094	0.032	4.13882	0.004806
6	1	2	3	1	0.098	0.034	4.36129	0.005968
7	1	3	1	3	0.093	0.020	4.45018	0.00801
8	1	3	2	1	0.078	0.030	4.67013	0.008936
9	1	3	3	2	0.096	0.031	4.56787	0.007951
10	2	1	1	2	0.121	0.030	4.56780	0.007843
11	2	1	2	3	0.112	0.030	4.28645	0.005579
12	2	1	3	1	0.12	0.030	4.48244	0.007161
13	2	2	1	3	0.126	0.030	4.47944	0.007082
14	2	2	2	1	0.120	0.04	4.61859	0.008186
15	2	2	3	2	0.125	0.042	4.53496	0.007306
16	2	3	1	1	0.108	0.03	4.99459	0.011512
7	2	3	2	2	0.098	0.028	4.83230	0.01019
18	2	3	3	3	0.108	0.03	4.68857	0.009085
19	3	1	1	3	0.148	0.042	4.57082	0.008148
20	3	1	2	1	0.140	0.042	4.74232	0.009177
21	3	1	3	2	0.154	0.05	4.72720	0.00901
22	3	2	1	1	0.160	0.051	4.84045	0.010659
23	3	2	2	2	0.157	0.052	4.79246	0.009215
24	3	2	3	3	0.156	0.05	4.54360	0.007634
25	3	3	1	2	0.14	0.038	5.22730	0.013004
26	3	3	2	3	0.128	0.04	5.01186	0.011422
27	3	3	3	1	0.132	0.04	5.18301	0.012274
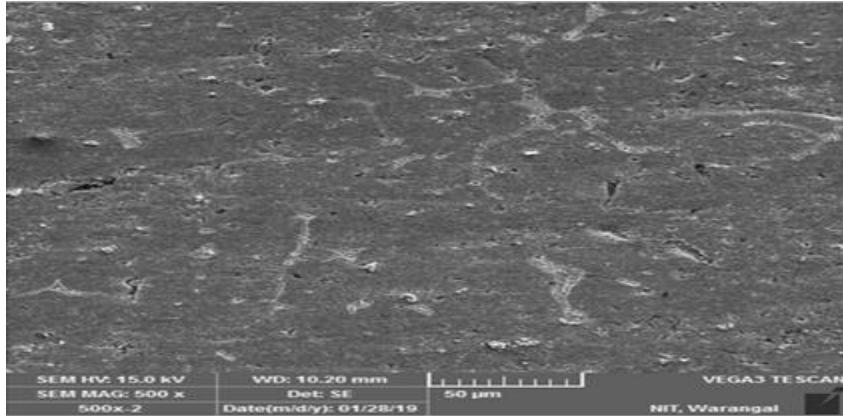
Figure 6 SEM image of machined surface of experimental run 3
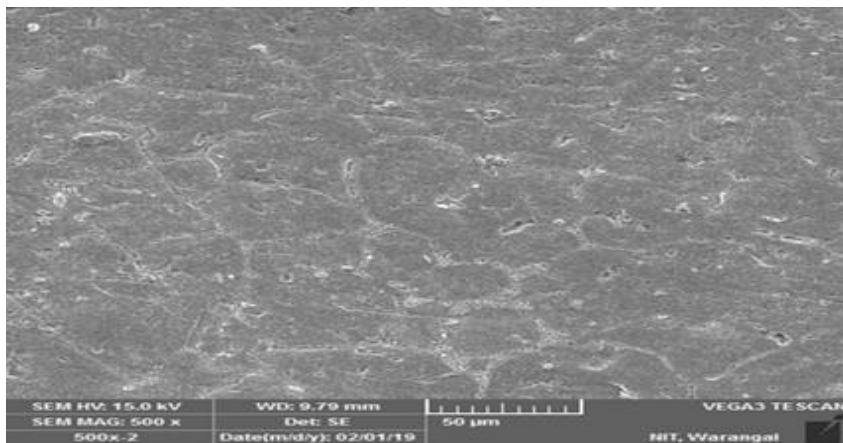
Figure 7 SEM image of machined surface of experimental run 14

4.Results and data analysis

The main goals of this work are to maximization of performance characteristic MRR and Minimization of the other three performance characteristics TWR, SR & SCD.

4.1 Influence of process parameters on MRR

Minitab16 software was used to plot the response (MRR) versus process parameters (P-On and I).

Figure 8 shows that MRR increases as pulse current increases due to an increase in discharge energy. MRR initially increases to a certain range in the case of P-On time, then decreases due to irregular discharges caused by the formation of a layer of ceramic SiC particles that acts as a shielding effect between the tool and the workpiece.
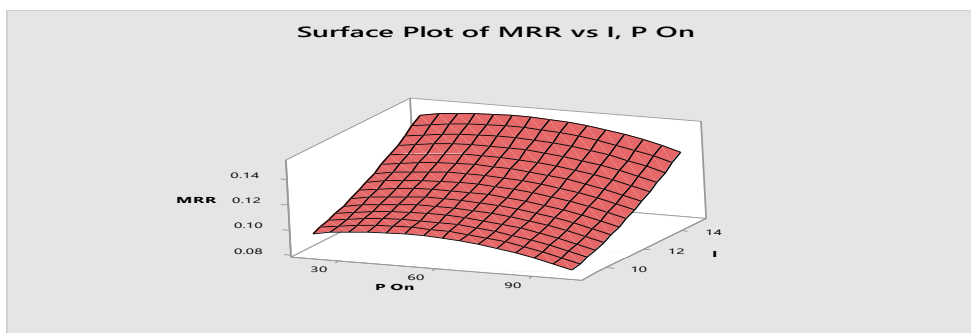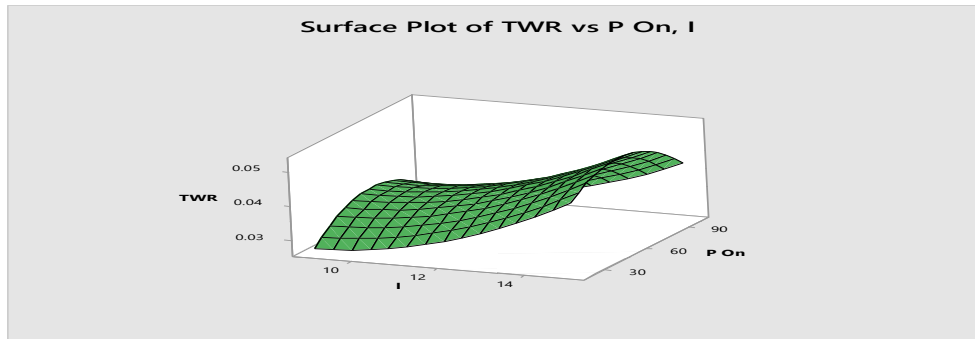

Figure 8 Surface plot of MRR Vs. I and P-On

4.2 Influence of process parameters on TWR

Minitab16 software was employed to plot the TWR response with a P-On and Current(I) process parameters. From the surface plot, *Figure 9*, it can be understood that TWR increases with an increase in pulse current due to an increase in the discharge energy, and also that leads to an increase in TWR.

Whereas for a Pulse On - time, TWR initially increases to a certain range than after it decreases. The discharges are irregular due to the formation of a layer of ceramic SiC particles and acts as a shielding effect between the tool and workpiece.

Figure 9 Surface plot for TWR Vs P-On and I

4.3 Influence of process parameters on SR and SCD

Minitab16 software was employed to plot the SR and SCD responses with P-On and Current(I) process parameters. From the surface plots in *Figure 10* and *Figure 11*, it can be understood that SR and SCD both

increase with an increase in pulse current and P-On due to an increase in the intensity of discharge energy and also increase in availability time of discharge energy.
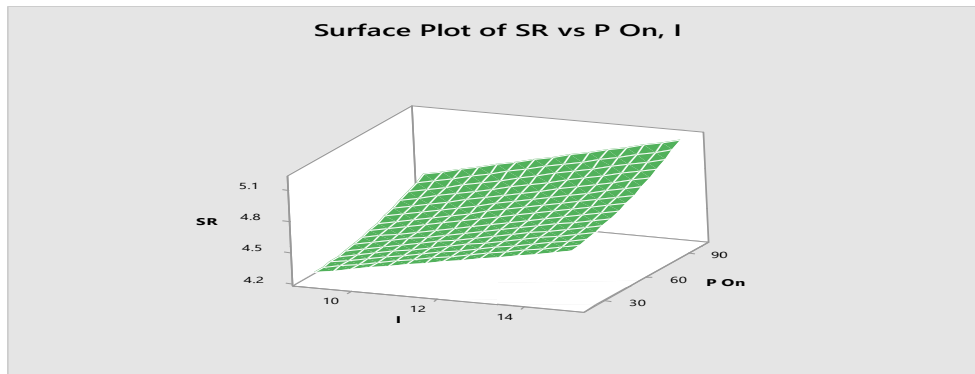
Figure 10 Surface plot of SR Vs. P-On and I
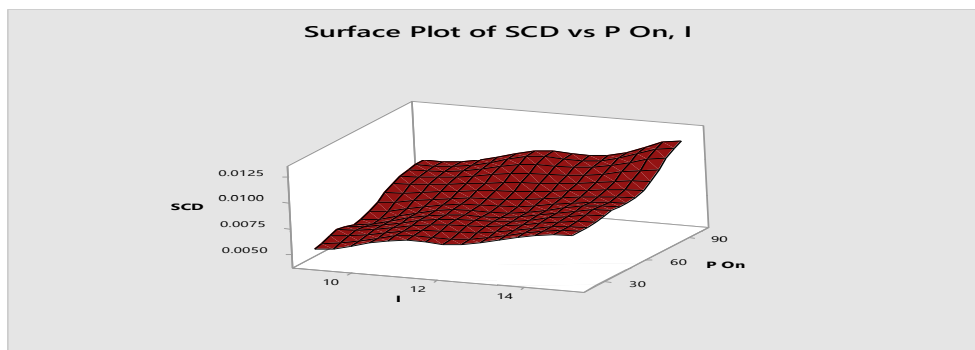
Figure 11 Surface plot for SCD Vs. P-On and I

4.4 Multi-response optimization

Multi-attribute optimization is executed by the TOPSIS method. The procedure is depicted by the following sequence of steps.

Step I: Develop a decision matrix that consists of 'n' number of responses and m number of alternatives and it is defined by the following matrix.

$$D_{i,j} = \begin{bmatrix} x_{11} & x_{12} & x_{13} & . & . & x_{1m} \\ x_{21} & x_{22} & x_{23} & . & . & x_{2m} \\ : & : & : & : & : & : \\ . & . & . & . & . & . \\ x_{n1} & x_{n2} & x_{n3} & . & . & x_{nm} \end{bmatrix}$$

Step II: The decision matrix is then normalized by the following expression (*Equation 3*) and tabulated in *Table 6*.

$$N_{ij} = \frac{x_{ij}}{\sqrt{\sum_{i=1}^n x_{ij}^2}} \quad where \; j = 1,2,3 \dots \dots, m \quad (3)$$

Step III: Evaluate weighted normalized matrix Uij by the following expression (*Equation 4*) and tabulated in *Table 7*.

$$U_{ij} = W_j * N_{ij} \tag{4}$$
$$\sum_{j=1}^n w_j = 1$$

Step IV: Determination of the positive and negative unique solutions from the following expressions (*Equation 5*).

$$U^+ = \left\{ \left[\left[\sum_i^{max} U_{ij} \, |j \epsilon J| \right], \left[\sum_i^{min} |j \epsilon J| i = 1,2, \dots. m \right] \right] \right\}$$
$$= \{u_1^+, u_2^+, u_3^+, \dots \dots u_n^+\} \tag{5}$$

$$U^- = \left\{ \left[\left[\sum_i^{min} U_{ij} \, |j \epsilon J| \right], \left[\sum_i^{max} |j \epsilon J| i = 1,2, \dots. m \right] \right] \right\}$$
$$= \{u_1^-, u_2^-, u_3^-, \dots \dots u_n^-\} \tag{6}$$

Step V: Calculating Euclidean distance from the unique positive and negative value (*Equation 7 and 8*) shown in *Table 8*.

$$E_i^+ = \sqrt{\sum_{j=1}^n \left[\left[u_{ij} - u_j^+ \right]^2 \right]} \quad i = 1,2\,3, .. m \quad (7)$$

$$E_i^- = \sqrt{\sum_{j=1}^n \left[\left[u_{ij} - u_j^- \right]^2 \right]} \quad i = 1,2\,3, ... m \quad (8)$$

Step VI: Calculating the nearness of the performance index by the following expression (Equation 9).

$$P_i = \frac{E_i^-}{E_i^+ + E_i^-} \quad i = 1,2,3, \dots, m \tag{9}$$

Step VII: Ranking is allocated according to the performance index from *Table 9*.

Whereas ideal positive, negative Euclidean values and corresponding performance index score characteristics of the TOPSIS method were evaluated in MS Excel 2007 software and by using *Equations 5,6,7,8, and 9* are represented in *Table 8* and *Table 9*. The maximum performance score is the relative closeness to the standard solution to achieve the optimal input parameters.

From *Table 9*, experiment number 1 encounters the highest score and it is ranked first. Machining of AL 6061 MMC on EDM to achieve the optimal input conditions are I-9, P-On20, P-Off50 and TL-1.5.

Table 6 Normalization matrix

Normalization			
MRR	TWR	SR	SCD
0.1680	0.1219	0.1772	0.1363
0.1648	0.1590	0.1787	0.1281
0.1458	0.1219	0.1707	0.0958
0.1711	0.1803	0.1854	0.1428
0.1490	0.1696	0.1726	0.1084
0.1553	0.1803	0.1818	0.1346
0.1474	0.1060	0.1855	0.1807
0.1236	0.1590	0.1947	0.2016
0.1521	0.1643	0.1905	0.1794
0.1917	0.1590	0.1904	0.1769
0.1775	0.1590	0.1787	0.1259
0.1902	0.1590	0.1869	0.1616
0.1997	0.1590	0.1868	0.1598
0.1902	0.2121	0.1926	0.1847
0.1981	0.2227	0.1891	0.1648
0.1711	0.1590	0.2082	0.2597

Normalization			
MRR	**TWR**	**SR**	**SCD**
0.1553	0.1484	0.2015	0.2299
0.1711	0.1590	0.1955	0.2050
0.2345	0.2227	0.1906	0.1838
0.2219	0.2227	0.1977	0.2070
0.2440	0.2651	0.1971	0.2033
0.2536	0.2704	0.2018	0.2405
0.2488	0.2757	0.1998	0.2079
0.2472	0.2651	0.1894	0.1722
0.2219	0.2015	0.2179	0.2933
0.2028	0.2121	0.2090	0.2577
0.2092	0.2121	0.2161	0.2769

Table 7 Weighted matrix

Weighted matrix			
MRR	**TWR**	**SR**	**SCD**
0.0420	0.0305	0.0443	0.0341
0.0412	0.0398	0.0447	0.0320
0.0364	0.0305	0.0427	0.0239
0.0428	0.0451	0.0463	0.0357
0.0372	0.0424	0.0431	0.0271
0.0388	0.0451	0.0455	0.0337
0.0368	0.0265	0.0464	0.0452
0.0309	0.0398	0.0487	0.0504
0.0380	0.0411	0.0476	0.0448
0.0479	0.0398	0.0476	0.0442
0.0444	0.0398	0.0447	0.0315
0.0475	0.0398	0.0467	0.0404
0.0499	0.0398	0.0467	0.0399
0.0475	0.0530	0.0481	0.0462
0.0495	0.0557	0.0473	0.0412
0.0428	0.0398	0.0521	0.0649
0.0388	0.0371	0.0504	0.0575
0.0428	0.0398	0.0489	0.0512
0.0586	0.0557	0.0476	0.0460
0.0555	0.0557	0.0494	0.0518
0.0610	0.0663	0.0493	0.0508
0.0634	0.0676	0.0505	0.0601
0.0622	0.0689	0.0500	0.0520
0.0618	0.0663	0.0474	0.0431
0.0555	0.0504	0.0545	0.0733
0.0507	0.0530	0.0522	0.0644
0.0523	0.0530	0.0540	0.0692

Table 8 Best and worst value

Euclidean distance from the ideal positive and negative value			
MRR	**TWR**	**SR**	**SCD**
0.0241	0.0570	0.0570	0.0570
0.0272	0.0525	0.0525	0.0525
0.0272	0.0639	0.0639	0.0639
0.0303	0.0468	0.0468	0.0468
0.0308	0.0549	0.0549	0.0549
0.0324	0.0478	0.0478	0.0478
0.0342	0.0519	0.0519	0.0519
0.0444	0.0376	0.0376	0.0376

Euclidean distance from the ideal positive and negative value			
MRR	TWR	SR	SCD
0.0363	0.0410	0.0410	0.0410
0.0292	0.0451	0.0451	0.0451
0.0245	0.0537	0.0537	0.0537
0.0267	0.0477	0.0477	0.0477
0.0251	0.0489	0.0489	0.0489
0.0384	0.0362	0.0362	0.0362
0.0369	0.0401	0.0401	0.0401
0.0487	0.0327	0.0327	0.0327
0.0436	0.0367	0.0367	0.0367
0.0372	0.0389	0.0389	0.0389
0.0372	0.0417	0.0417	0.0417
0.0416	0.0356	0.0356	0.0356
0.0485	0.0381	0.0381	0.0381
0.0553	0.0353	0.0353	0.0353
0.0514	0.0382	0.0382	0.0382
0.0444	0.0439	0.0439	0.0439
0.0567	0.0308	0.0308	0.0308
0.0509	0.0270	0.0270	0.0270
0.0548	0.0270	0.0270	0.0270

Table 9 Ranking of the performance index

Performance scores (Pi)	Rank
0.7031	1
0.6593	5
0.7013	2
0.6068	9
0.6406	7
0.5962	11
0.6028	10
0.4585	19
0.5308	12
0.6073	8
0.6870	3
0.6409	6
0.6608	4
0.4848	17
0.5207	14
0.4018	23
0.4568	20
0.5110	15
0.5289	13
0.4613	18
0.4396	21
0.3898	24
0.4263	22
0.4974	16
0.3520	25
0.3466	26
0.3298	27

4.5 Data analysis

To measure the influence of process parameters of Die-Sink EDM on Al MMC, 27 experimental tests were conducted (L27 orthogonal array). The responses were recorded and further multi-response optimization was attempted with the aid TOPSIS method. Here the goals are Maximization of MRR, Minimization of TWR, SR, and SCD. It has been explored that the required goal of achieving the optimal combination parameters. Then after TOPSIS method is mingled

747

with the ANOVA for obtaining the favorable optimal machining conditions. Main effect plots were drawn and represented in *Figure 12*. From the main effect plot, it has been discovered that as current and pulse on increases performance score decreases, but for tool lift and pulse off performance score primarily decreases and then increases.

It is because of the generation of carbide layer in-between tool and workpiece (spark gap). By observing the response for means it can be concluded that the major influence on performance score is current and pulse on time after that it is followed by P-Off and Tool lift (*Table 10*).

Table 10 Response of means of a performance score

Level	I	P-On	P-Off	TL
		Performance score		
1	0.6110	0.6032	0.5392	0.4962
2	0.5523	0.5359	0.5135	0.5111
3	0.4191	0.4433	0.5297	0.5751
Delta	0.1919	0.1598	0.0258	0.0789
Rank	1	2	4	3

The prediction of the Responses (R_p) of the EDM parameters can be evaluated by the following equation 10:

$$R_P = R_{mean} + \sum_{i=1}^{m}(R_i - R_{mean}) \qquad (10)$$

Where
R_p is the response to be predicted
R_{mean} is mean of a mean of the response
R_i is the mean response of ith parameter
m is the number of input parameters.

The present investigation reveals the significant influence of input process parameters on output responses. The most optimal input parametric conditions of the EDM process for acquiring maximum MRR and minimum TWR, SR, and SCD are achieved by the TOPSIS method and presented in *Table 11*.
The most significant factors affecting the performance

score, according to *Table 12*, are peak current and P-On time, followed by tool lift. The P-Off factor had a minor impact on the response performance score, which is consistent with the literature [39]. A peak current input level of 9 Amps, P-On time input level of 20 s, P-Off time input level of 50 s, and Tool Lift input level of 4.5 s are predicted to be optimal machining conditions. The results of the confirmatory tests were 0.103 g/min MRR, 0.022 g/min TWR, 4.108 m SR, and 0.0048213 m SCD, as shown in *Figure 13*. It has also been verified that the deviation from the average performance score is 1.78 percent, and that it is highly interactive and accurate, i.e., with confidence.

Complete list of abbreviations is shown in Appendix I.
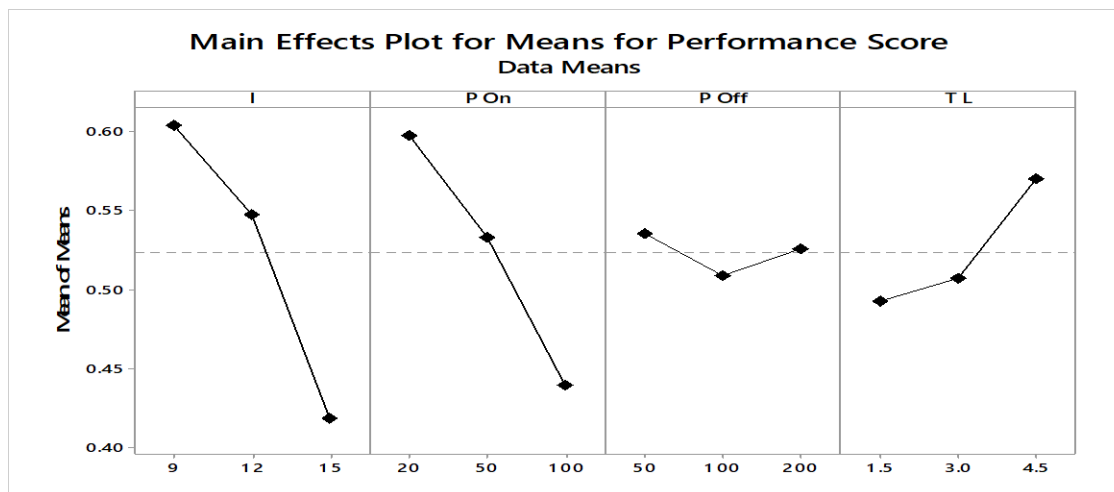
Figure 12 Main Effect plot for means of the Performance score

Table 11 Predicted and experimental values by TOPSIS method

Response	Experimental Response Values (I1-POn1-POff1-TL3)
MRR	0.103 gm/min
TWR	0.022 gm/min
SR	4.108 µm
SCD	0.004821µm
Performance index score (Pi)	0.7328
Predicted Performance index score from ANOVA	0.7461
Deviation	1.78%

Table 12 ANOVA for means of performance score

ANOVA Table for Means of Performance Score					
Source	DOF	SS	MSS	F-ratio	% of Contribution
I	2	0.1741	0.0870	87.00	50.7288
P-On	2	0.1159	0.0579	57.92	33.8192
P-Off	2	0.0030	0.0015	1.53	0.8746
TL	2	0.0316	0.0158	15.82	9.3294
Residual Error	18	0.0180	0.0010		5.2478
Total	26	0.3428			100

F ratio from the table with the significance level of 0.05 and DOF (2, 18) is 3.55.
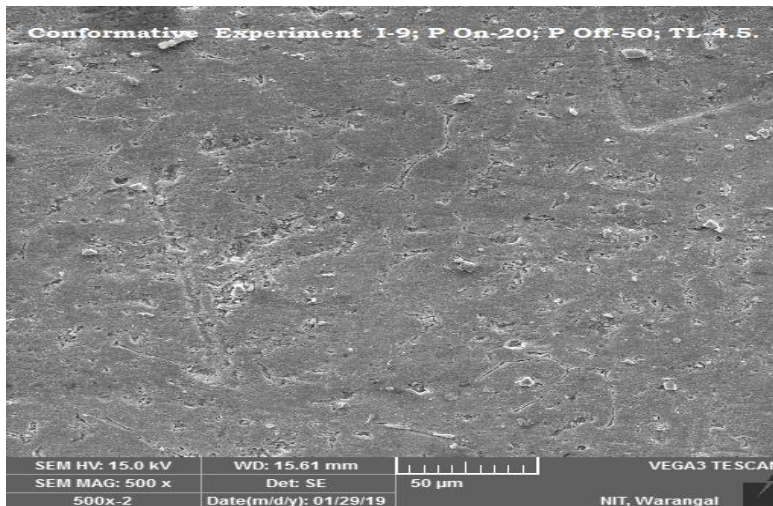
Figure 13 SEM Photograph of machined surface for validation

Limitations

The limitations of the above work are as follows
1. The effect of high temperature on metallurgical aspects during machining on work surface.
2. The development of residual stress on the work sample machined surface.

The EDM process causes these limitations. The transfer of high thermal energy during machining on the work sample is the mechanism of EDM machining. During P-On time, there is a sudden heating due to high thermal energy, and during P-Off and TL time, there is a flushing of dielectric fluid causes quenching of the work surface, resulting in high residual stresses and metallurgical changes.

5.Conclusion

In this work, a study was executed to investigate the multi-response optimization of EDM process parameters in the machining of SiC and B4C particle reinforced Al-6061 HMMC by application of the TOPSIS method. Minitab software is employed for surface plots and it reveals that the maximum of MRR

as 0.160 gm/min is obtained at process parameters settings of I-15 Amps, P-On-50 μs, P-Off- 50 μs, and TL-1.5 s, the minimum of TLWR as 0.0203 gm/min is achieved at process parameters settings of I-9 Amps, P-On-100 μs, P-Off- 50 μs and TL-4.5 s and minimum of SR of 4.094 μm and SFCD of 0.0042 μm were attained at process parameters settings of I-9 Amps, P-On-20 μs, P-Off- 200 μs, TL-4.5 s. TOPSIS multi-objective optimization reveals the significant impact of process parameters on output performances. Peak current and P-On are very significant factors that affect the responses performance score. It is due to the availability of high thermal energy from spark discharges. During tool lift time, the shielding layer of ceramic particles and debris is flushed away by dielectric fluid between the tool and workpiece. Thus, TL is also a significant parameter on responses performance score. The most optimal input parametric conditions of the EDM process for acquiring maximum MRR as 0.103 gm/min and minimum TWR as 0.022 gm/min, SR 4.108 μm and SCD as 0.0048 μm were achieved at I-9 Amps, P-On-20 μs, P-Off-50 μs, and TL-4.5 s. The prediction responses performance score and experimental responses performance score has a very less deviation of 1.78% which is very highly interactive and also within the confidence level. This study will be beneficial to the production industries in choosing effective machining conditions of a novel Hybrid MMC of the die-Sink EDM for manufacturing the components in modern engineering applications like ship buildings, aerospace, and automobile applications.

The following work can be attempted in future in the following ways:
1. The influence metallurgical aspects of generated temperature during machining on work surface.
2. The influence sudden heating and quenching on residual stresses.
3. Influence of temperature on machining and work life. So more sensors are arranged to measure temperature at each level of machining.

Acknowledgment

Conflicts of interest
The authors have no conflicts of interest to declare.

References
[1] Chawla KK. Composite materials: science and engineering. Springer Science & Business Media; 2012.

[2] Garg A, Lam JS. Modeling multiple-response environmental and manufacturing characteristics of EDM process. Journal of Cleaner Production. 2016; 137:1588-601.

[3] Nayim ST, Hasan MZ, Jamwal A, Thakur S, Gupta S. Recent trends & developments in optimization and modelling of electro-discharge machining using modern techniques: a review. In AIP conference proceedings 2019. AIP Publishing LLC.

[4] Rao CS, Rao GA, Selvaraj N, Bose PS, Chandramohan VP. Mechanical engineering for sustainable development: state-of-the-art research. CRC Press; 2019.

[5] Bodukuri AK, Eswaraiah K, Rajendar K, Pradeep V. Investigation of optimum compacting parameters for aluminium, SiCP and B4C composites. Materials Today: Proceedings. 2018; 5(13):26866-72.

[6] Poovazhagan L, Kalaichelvan K, Sornakumar T. Processing and performance characteristics of aluminum-nano boron carbide metal matrix nanocomposites. Materials and Manufacturing Processes. 2016; 31(10):1275-85.

[7] Aruna K, Diwakar K, Bhargav Kumar K. Development and characterization of Al6061-ZrO2 reinforced metal matrix composites. International Journals of Advanced Research in Computer Science and Software Engineering. 2018; 8:270–5.

[8] Poria S, Sahoo P, Sutradhar G. Tribological characterization of stir-cast aluminium-TiB 2 metal matrix composites. Silicon. 2016; 8:591-9.

[9] Rino JJ, Sivalingappa D, Koti H, Jebin VD. Properties of Al6063 MMC reinforced with zircon sand and alumina. IOSR Journal of Mechanical and Civil Engineering. 2013; 5(5):72-7.

[10] Lee SH, Li XP. Study of the effect of machining parameters on the machining characteristics in electrical discharge machining of tungsten carbide. Journal of Materials Processing Technology. 2001; 115(3):344-58.

[11] Kumar H, Davim JP. Role of powder in the machining of Al-10% SiCp metal matrix composites by powder mixed electric discharge machining. Journal of Composite Materials. 2011; 45(2):133-51.

[12] Singh PN, Raghukandan K, Rathinasabapathi M, Pai BC. Electric discharge machining of Al–10% SiCP as-cast metal matrix composites. Journal of Materials Processing Technology. 2004; 155:1653-7.

[13] Hung NP, Yang LJ, Leong KW. Electrical discharge machining of cast metal matrix composites. Journal of materials processing technology. 1994; 44(3-4):229-36.

[14] Liao HC, Chen YK. Optimizing multi-response problem in the taguchi method by DEA based ranking method. International Journal of Quality & Reliability Management. 2002; 19(7):825-37.

[15] Vaddi VR, Ch SR, Bushaboina SK, Banka H. Application of TOPSIS with taguchi method for multi-attribute optimization of machining parameters in EDM. International conference on advances in design, materials, manufacturing and surface engineering for mobility. 2018.

[16] Rui-song J, Wen-hu W, Guo-dong S, Zeng-qiang W. Experimental investigation on machinability of in situ formed TiB2 particles reinforced Al MMCs. Journal of Manufacturing Processes. 2016; 23:249-57.

[17] Bodukuri AK, Eswaraiah K, Rajendar K, Sampath V. Fabrication of Al–SiC–B4C metal matrix composite by powder metallurgy technique and evaluating mechanical properties. Perspectives in Science. 2016; 8:428-31.

[18] Pradhan S, Ghosh S, Barman TK, Sahoo P. Tribological behavior of Al-SiC metal matrix composite under dry, aqueous and alkaline medium. Silicon. 2017; 9:923-31.

[19] Das S, Chandrasekaran M, Samanta S, Kayaroganam P, Davim P. Fabrication and tribological study of AA6061 hybrid metal matrix composites reinforced with SiC/B4C nanoparticles. Industrial Lubrication and Tribology. 2019; 71(1):83-93.

[20] Reddy PS, Kesavan R, Ramnath BV. Investigation of mechanical properties of aluminium 6061-silicon carbide, boron carbide metal matrix composite. Silicon. 2018; 10:495-502.

[21] Das S, Chandrasekaran M, Samanta S. Comparison of mechanical properties of AA6061 reinforced with (SiC/B4C) micro/nano ceramic particle reinforcements. Materials Today: Proceedings. 2018; 5(9):18110-9.

[22] Vijayabhaskar S, Rajmohan T, Sisir TP, Abishek JP, Reddy RM. Review of WEDM studies on metal matrix composites. In IOP conference series: materials science and engineering 2018 (pp. 1-6). IOP Publishing.

[23] Muthuramalingam T, Mohan B. Multi-response optimization of electrical process parameters on machining characteristics in electrical discharge machining using taguchi--data envelopment analysis-based ranking methodology. Journal of Engineering & Technology. 2013; 3(1):57-60.

[24] Muniappan A, Jaivaakheish AP, Jayakumar V, Arunagiri A, Senthilkumar R. Multi objective optimization of process parameters in WEDM of aluminum hybrid composite using taguchi and topsis techniques. In IOP conference series: materials science and engineering 2018 (pp.1-10). IOP Publishing.

[25] Manoj M, Jinu GR, Muthuramalingam T. Multi response optimization of AWJM process parameters on machining TiB 2 particles reinforced Al7075 composite using Taguchi-DEAR methodology. Silicon. 2018; 10:2287-93.

[26] Patel JD, Maniya KD. A review on: wire cut electrical discharge machining process for metal matrix composite. Procedia Manufacturing. 2018; 20:253-8.

[27] Patil IS, Rao SS, Herbert MA, Goudar DM. Experimental investigation and optimisation of mechanical and microstructure behaviour of stir cast and hot-pressed Al-12.5% Si-ZrO2 composites: taguchi and super ranking concept. Advances in Materials and Processing Technologies. 2021:1-27.

[28] Srivastava AK, Sharma B, Saju BR, Shukla A, Saxena A, Maurya NK. Effect of Graphene nanoparticles on microstructural and mechanical properties of aluminum based nanocomposites fabricated by stir casting. World Journal of Engineering. 2020; 17(6):859-66.

[29] Mouralova K, Kovar J, Klakurkova L, Bednar J, Benes L, Zahradnicek R. Analysis of surface morphology and topography of pure aluminium machined using WEDM. Measurement. 2018; 114:169-76.

[30] Kumar H, Manna A, Kumar R. Modeling of process parameters for surface roughness and analysis of machined surface in WEDM of Al/SiC-MMC. Transactions of the Indian Institute of Metals. 2018; 71:231-44.

[31] Palanisamy D, Devaraju A, Manikandan N, Balasubramanian K, Arulkirubakaran D. Experimental investigation and optimization of process parameters in EDM of aluminium metal matrix composites. Materials Today: Proceedings. 2020; 22:525-30.

[32] Rizwee M, Rao PS. Analysis & optimization of parameters during EDM of aluminium metal matrix composite. Journal of University of Shanghai for Science and Technology. 2021; 23(3):218-23.

[33] Rizwee M, Minz SS, Orooj M, Hassnain MZ, Khan MJ. Electric discharge machining method for various metal matrix composite materials. International Journal of Innovative Technology and Exploring Engineering. 2019; 8(9):1796-807.

[34] Rizwee M, Rao PS, Khan MY. Recent advancement in electric discharge machining of metal matrix composite materials. Materials Today: Proceedings. 2021; 37:2829-36.

[35] Pandey S, Shrivastava PK. Vibration-assisted electrical arc machining of 10% B4C/Al metal matrix composite. Proceedings of the Institution of Mechanical Engineers, Part C: Journal of Mechanical Engineering Science. 2020; 234(6):1156-70.

[36] Phate M, Toney S, Phate V. Modelling and investigating the impact of EDM parameters on surface roughness in EDM of Al/Cu/Ni alloy. Australian Journal of Mechanical Engineering. 2020:1-4.

[37] Nguyen HP, Ngo NV, Nguyen QT. Optimizing process parameters in edm using low frequency vibration for material removal rate and surface roughness. Journal of King Saud University-Engineering Sciences. 2021; 33(4):284-91.

[38] Singh T, Arya RK, Dvivedi A. Experimental investigations into rotary mode electrochemical discharge drilling (RM-ECDD) of metal matrix composites. Machining Science and Technology. 2020; 24(2):195-226.

[39] Singh M, Maharana S. Investigating the EDM parameter effects on aluminium based metal matrix composite for high MRR. Materials Today: Proceedings. 2020; 33:3858-63.

[40] Chen Z, Zhou H, Yan Z, Han F, Yan H. Machining characteristics of 65 vol.% SiCp/Al composite in

micro-WEDM. Ceramics International. 2021; 47(10):13533-43.

Mr. Anil Kumar Bodukuri, Scholar, in Mechanical Engineering. He did his master's at the National Institute of Technology, Warangal, Telangana, India. He is working as Faculty in the Department of Mechanical Engineering at University College of Engineering and Technology, Kakatiya University, Warangal, India. He published 6 research papers in the Scopus index journal and nearly 8 papers in a national and international conference in the field of Mechanical Engineering. He is perusing his Ph.D. at Kakatiya University.
Email: anil.kucet@gmail.com

Dr. Eswaraiah Kesha is a Professor and Head of the Department of Mechanical Engineering at Kakatiya Institute of Technology and Science Warangal, Telangana state, India. He did his Ph.D. at the National Institute of Technology, Warangal. His research areas are Machining and Optimization in Mechanical Engineering. He published many research papers in reputed journals like SCI and Scopus Indexed.
Email: eswaraiah_kits@yahoo.com

Appendix I

S.No.	Abbreviation	Description
1	ANOVA	Analysis of Variance
2	B4C	Boron Carbide
3	CP	Current Peak
4	DEAR	Data Envelopment Analysis Ranking
5	DOE	Design of Experiments
6	DOF	Degrees of Freedom
7	EDM	Electric Discharge Machine
8	EDS	Energy-dispersive Spectroscopy
9	EDX	Energy-dispersive X-ray Spectroscopy
10	FESEN	Field Emission Scanning Electron Nicroscope
11	GRA	Grey Relational Analysis
12	HMMC	Hybrid Metal Matrix Composite
13	I	Pulse Current
14	MMC	Metal Matrix Composite
15	MRR	Metal Removal Rate
16	OA	Orthogonal Array
17	P-Off	Pulse Off duration
18	P-On	Pulse On duration
19	PSO	Particle Swarm Optimization
20	Rp	Responses
21	RSA	Response Surface Methodology
22	SCD	Surface Crack Density
23	SEM	Scanning Electron Microscope
24	SiC	Silicon Carbide
25	S/N	Signal to Noise ratio (K)
26	SR	Surface Roughness
27	SVR	Support Vector Regression
28	TL	Tool Lift time
29	TOPSIS	Technique of Order Preference Similarity to the Ideal Solution
30	TWR	Tool Wear Rate
31	WEDM	Wire cut Electric Discharge Machine
32	WR	Wear Ratio